www.nature.com/scientificreports

scientific reports

Check for updates

OPEN

Reducing noise levels in eddy current measurements using self-differential probes of the substrate conductivity under a layer of conductive coating in moved objects

Volodymyr Ya. Halchenko, Ruslana Trembovetska & Volodymyr Tychkov✉

In the research, the method of reducing the levels of all noises caused by uncontrollable interfering factors has been generalized and extended to surface eddy current conductivity meters of the substrate under a layer of non-ferromagnetic metal coating. The method is applied at the probe design stage as a result of Taguchi's optimization search for a combination of ECP parameters that reduces the influence of noise factors. The designs of self-differential UECPs were analyzed. Dynamic measurements of substrate conductivity were considered. Variants of TO structures with non-magnetic and weakly magnetic substrates were investigated, i.e., eddy current conductivity measurements were extended to objects with weakly magnetic substrates. As a result of confirmatory experiments, the effectiveness of the obtained optimal combinations of parameters for both variants of TO structures was proven. The option with rectangular coils was selected as the one with the maximum SNR among the optimized alternative designs of the ECP. The variance analysis established the ranks of the influence of the measuring parameters on the SNR. The statistical significance of the analyzed parameters was determined. The Monte Carlo numerical-experimental method demonstrated the advantages of optimal designs, which are characterized by lower signal variability under the influence of noise factors.

Keywords Eddy current conductivity measurements, Non-magnetic and weakly magnetic substrate, Metal coating, Moved object, Noise reduction, Taguchi`s optimization method, Variance ANOVA analysis of parameter effects

Abbreviations

ECT	eddy current testing
TO	tested object
ECP	eddy current probe
SNR	ratio signal-to-noise
DOE	design of experiment
DSP	digital signal processing
UECP	uniform eddy current probe
EMF	electromotive force
ANOVA	analysis of variance

Relevance of the Research

The measurement of electrical conductivity in materials and components is crucial in industrial processes. This parameter serves as a specific indicator of changes in material properties, enabling the estimation of product

Department of Instrumentation, Mechatronics and Computerized Technologies, Cherkasy State Technological University, 460 Shevchenko Blvd, Cherkasy 18006, Ukraine. ✉email: v.tychkov@chdtu.edu.ua

condition and quality, and ensuring their reliability in various industries. This problem is not easy even for tested objects (TO) made of homogeneous material and kept in a static state[1]. If the TO has a structure with a conductive coating applied to the substrate, and if it is moved, the problem complexity of measuring the conductivity of the substrate under the coating layer increases significantly. However, the actuality of solving this problem is obvious. Estimating material degradation after heat treatment based on conductive properties, inspecting TO with anodized surfaces or other protective coatings, including anti-corrosion coatings, are just a few of the many examples of practical applications for the results of such measurements. The introduction should not include subheadings.

The use of the eddy current testing method to achieve this goal poses certain difficulties. It can be argued that this problem is, in a sense, intermediate between measuring the conductivity of objects made of a one single material and measuring the thickness of coatings of essentially two-layer TOs, but it has its own peculiarities. In addition to the traditional problems characteristic of measuring the conductivity of non-magnetic materials, in particular, lift-off changes and local variations in the conductivity of the surface layer, which are typical for two-layer TOs, there are additional specific problems. Noise factors that also interfere with measurements include the variability of the thickness of the TO metal coating. For two-layer objects with a weakly magnetic substrate, noises also cause local variations in their magnetic permeability. Also, when measuring on moved TOs, it is necessary to take into account additional eddy currents caused by their movement at a certain speed. Thus, the output signal of the eddy current probe (ECP) during measurements is formed as a result of the interaction of the electromagnetic excitation field with the substrate and coating materials, as well as the action of all the additional factors mentioned above.

There are two problems to be solved in order to obtain acceptable results during measurements. Firstly, it is the extraction of information about the conductivity of the substrate from the selected signal. Secondly, in order to effectively perform the first problem, it is necessary to determine the substrate parameter in the presence of the coating as accurately and consistently as possible. This article discusses the implementation of this particular problem, which consists of reducing noise levels and increasing the signal-to-noise ratio.

State-of-the-art

Currently, there is a well-known set of practical techniques, including constructive, hardware, methodological, signal processing, calibration, etc., which are actually used for this purpose in industrial measurement systems[2,3]. We will analyze them, identifying and emphasizing existing drawbacks. Among the design solutions, self-differential and self-nulling probes have gained popularity and widespread use, as reflected, for example, in studies[4–7], which remove the common-mode component of the signal and are effective in reducing the influence of lift-off and macro-relief of the TO surface. However, they do not overcome measurement obstacles caused by the electrophysical properties of TO. A common variant of ECP designs is their modifications with cores[8–10], in particular ferrite Pot-core or E-core, which are capable of concentrating the excitation field, shielding background magnetic interference, and increasing sensitivity to deeper layers of material, thereby increasing the *SNR*. However, such probes cannot be used at high temperatures of the environment due to the corresponding instability. The essential elements of the ECP design that affect the *SNR* level[11,12] are the geometry and form-factor of their coils, setting their optimal dimensions to ensure maximum sensitivity to the conductivity of the substrate material. This approach requires multi-objective optimization, which involves the need to prioritize individual criteria when making compromises, which is not always acceptable without losing the accuracy of substrate conductivity measurements.

An important factor in obtaining a signal that is "clean" from noise is the adequate selection of frequency modes for exciting the probes, i.e., adapting the excitation parameters to the measurement problem. Single-frequency excitation and broadband multi-frequency methods, in particular sweep-frequency[13,14] and pulsed methods[15–19], are widely used. For single-frequency excitation, the optimal frequency ensures the skin depth of the electromagnetic field penetrates to the substrate metal, while not being too low in order to achieve a high *SNR*[2]. Multi-frequency excitation, including pulsed PEC, allows distinguishing contributions to signals from different depths of the TO and is characterized by rather high noise suppression capabilities, but this occurs as a result of processing their already selected values after measurements[20]. However, it is advisable to implement the invariance of probe signals to noise at the stage of their formation.

Noise reduction is also achieved through the use of appropriate schematic design, in particular, low-noise preamps, analog filters, etc., and digital signal processing (DSP) (ensemble averaging, band-pass filters, wavelet shrinkage, lock-in or synchronous detection at a given frequency, etc.)[21–23]. These tools are quite effective in eliminating noise, both electronic noise and, more importantly, noise caused by specific properties of the TO or measurement conditions in certain situations. In the vast majority of cases, measurements require their comprehensive application, which can be considered a drawback.

Methods developed in recent years for denoising and *SNR* improvement of ECP signals based on machine learning deserve special attention[24–27]. In particular, the denoising autoencoder[28] uses unsupervised deep learning to clean up impulse eddy current responses of probes, while[29] uses ML-oriented denoising computational algorithms aimed at improving *SNR*. The noise influence of lift-off was predicted using various methods, including partial least squares regression, support vector machine regression, and convolutional neural networks. The advantages of a neural network option that is trained and optimized using data calculated on the theoretical TREE model proposed by Theodoulidis have been identified. Considering all the advantages of the machine learning approach, it should be noted that they are achieved at the signal processing stage, which is not always acceptable.

The approach proposed by the authors of the article in studies[30–33] provides a signal with a high *SNR* value and significantly lower variations under the influence of lift-off changes, geometry instability, and local electrophysical noise deviations from the norm in the materials of the TO structure. It provides for implementation at the theoretical and experimental level, which is aimed at optimizing the search using the Taguchi method for the design and operating parameters of probes on the DOE obtained, including by computer modeling using mathematical models of the direct problem and orthogonal arrays. The found optimum provides the maximum *SNR* together with the minimum variance of output signals, determined by the combination of all specified noise factors, within the selected ECP design. The approach was used for robust parameter design of surface probes for measuring the conductivity of thick objects and plate thickness gauges, and proved to be effective, as interference-free signals are obtained at the stage of their formation. It seems promising for solving the problem mentioned in this article.

Therefore, despite the noticeable progress observed in modern approaches to noise suppression in eddy current measurements, the analyzed techniques do not fully solve this problem. In most cases, this is achieved at the stage of processing signals already selected from probes. The instruments used do not allow simultaneous suppression of the entire range of noises, but are tuned only to certain types of noise or, at best, to some of their combinations. The Taguchi optimization method, which aims to overcome these drawbacks for certain types of eddy current measurements, takes a somewhat distinct position in this regard, but it requires further development for the problem formulated in the article.

Main attributes of the research

The object of this research is the process of eddy current measurements of the electrical conductivity of the substrate under a layer of metal coating using a surface probe.

The subject of research is a method for simultaneous suppression of all types of noise most significant for such measurements, caused by both the conditions of their conduct and the properties of the moved TO, which is implemented as a result of Taguchi's robust parameter design of optimal probe designs and ensures noise reduction during signal formation, rather than after their selection.

The purpose of this article is to develop a method for maximizing *SNR* and, accordingly, reducing the noises level of surface self-differential eddy current conductivity meters of non-magnetic and weakly magnetic substrates under a layer of metal coating of a moved object, caused by a combination of simultaneous changes in lift-off, geometric inconsistencies, local noise deviations from the norm of the electrophysical properties of coating materials and the substrate of the TO, as a result of an optimization search for the design and operating parameters of the ECP of a priori selected design.

The main scientific contributions of this study are as follows:

- The method of noise reduction proposed earlier by the authors, the advantage of which is its application at the design stage, which ultimately ensures the selection of noise-free signals directly from the probes without additional processing, has been generalized and extended to surface self-differential eddy current conductivity meters for non-magnetic and weakly magnetic substrates under a layer of metal coating of moved object.
- Taking into account all the characteristics inherent in these dynamic measurements, in particular, the generation of additional eddy currents caused by the movement of the TO at a certain speed.
- Extension of eddy current conductivity measurements with TO with a non-magnetic substrate, as is usually the case, to objects with weakly magnetic properties.
- Selecting the design of the ECP with rectangular coils from among their optimized self-differential variants for maximum *SNR*.
- Determination, as a result of variance ANOVA analysis, of ranked orders of parameters affecting the signal-to-noise ratio, verification of their significance using statistical methods based on Fisher's criterion.
- Numerical-experimental verification using the Monte-Carlo method of the optimal parameter combinations of substrate conductivity meters found to suppress output signal variations under noise effects, both individual interference and their combination.

The structure of the article is as follows: in section «Theoretical modeling and robust parameter design» include subsections «Research on the energy levels of signals from meters with competitive excitation systems», «Taguchi's robust parameter design methodology for finding optimal designs for meters», «Research on the energy levels of signals from meters with competitive excitation systems», «Taguchi's design of experiments for rectangular coils meters», «Taguchi's design of experiments for tangential meters», «Comparative analysis based on the *SNR* criterion of optimal designs for conductivity meters», «Confirmatory experiment to establish the optimality of the meter design», «Variance ANOVA-analysis of the influence of meter parameters on *SNR*», «Numerical-experimental research of signal variability in meters using the Monte-Carlo method» and section «Conclusions».

Theoretical modeling and robust parameter design

Research on the energy levels of signals from meters with competitive excitation systems

Selecting the design of probes for eddy current conductivity measurements is one of the most important tasks that requires effective decisions to be made among known alternatives in conditions of information uncertainty. Having certain knowledge about the advantages and disadvantages of a number of ECP designs, it is necessary to choose one that has high sensitivity to the measured value, a significant signal level, certain design features, etc. An analysis of promising directions for the creation of new probe designs led to a focus on self-differential or self-nulling surface transformer variants[34,35]. In these researches, two modifications of such designs were selected, which represent uniform eddy current probes (UECP) with orthogonal coils. The first type of design includes a rectangular excitation coil, which is located in parallel to the object of measurement. The pick-up coil of this design is also rectangular and is characterized by a perpendicular orientation relative to the TO surface. The second type also has a rectangular excitation coil, but it is oriented perpendicular to the TO surface. Such a probe excitation system generates an electromagnetic field tangential to the TO surface, unlike the first design, where its direction is normal to the surface. In this design, the pick-up coil has a cylindrical form-factor and is placed parallel to the TO surface. In both cases, self-differential eddy current probes with a single pick-up coil function as self-balanced systems, in which the induced signals represent the gradient of locally generated EMF in their semi-segments. The designs primarily ensure suppression of insignificant lift-off noises[35], mutual compensation of the influence of coating layers and surface inhomogeneity, and improved sensitivity to conductivity changes.

Let us explain the principle of operation of such probes using the example of an ECP with rectangular coils. Let us assume that two identical semi-segments, symmetrically located relative to the Oz axis (Fig. 1), together form a pick-up coil. If the centre-to-centre distance between the coils is $c=0$ and the tested object is stationary $v=0$, then the EMFs induced in the semi-segments by eddy currents compensate each other. This is due to the symmetry of the distribution of eddy currents density under the semi-segments of the pick-up coil in a conductive environment that is uniform in terms of its electrophysical properties. Therefore, due to the intrinsic self-differential property of the design, the resulting EMF of the probe is zero. When $v\neq 0$, the tested object is moving and the density of eddy currents is redistributed under the semi-segments of the pick-up coil, with a higher concentration under one of them. Therefore, the balance of the EMF of the semi-segments is disturbed and, accordingly, a differential signal is formed, which is proportional to their difference. This is caused by the asymmetry of the resulting electromagnetic field and, accordingly, the difference in the distribution of the x-component magnetic flux density B_x. Therefore, the coil responds to the field gradient, and even relatively small changes in the conductivity of the substrate have a significant effect on the probe signal. Schematic designs of uniform self-differential ECPs with orthogonal coils are shown in Fig. 1.

Therefore, further research was focused on modeling the measurement processes of both types of ECPs located above moved TOs with coatings of various non-magnetic materials applied to them. Numerical experiments were conducted for non-magnetic and weakly magnetic substrates under all other equal conditions. The best design was selected based on a comparative analysis of the modeled output signal levels of both types of designs. That is, the higher energetic level of the signal is decisive for conclusions about the effectiveness of the design. Mathematical models of probes for calculating induced EMF at sinusoidal excitation $Ie^{j\omega t}$ with angular frequency ω are as follows.

The first one is designed for ECPs with multi-turn rectangular coils[34]

$$E=\frac{2\omega\mu_0 I N_1 N_2}{\pi^2 w_1 h_1 w_2 h_2}\int\limits_{-\infty}^{\infty}\int\limits_{-\infty}^{\infty}\frac{\kappa k_1 k_2}{\eta^2\xi\varsigma^2}\sin\left(\frac{h_2\xi}{2}\right)e^{-j\xi c}\cdot\left[e^{-(2z_1+w_2+a_2)\varsigma}-e^{-(2z_1+w_2+a_2+h_1)\varsigma}\right]d\xi d\eta \qquad (1)$$

In the Eq. (1)

$$\kappa=\frac{\left(\frac{\gamma_1}{\varsigma}-\frac{\mu_1}{\mu_0}\right)\cdot\left(\frac{\gamma_2}{\gamma_1}+\frac{\mu_2}{\mu_1}\right)+\left(\frac{\gamma_1}{\varsigma}+\frac{\mu_1}{\mu_0}\right)\cdot\left(\frac{\gamma_2}{\gamma_1}-\frac{\mu_2}{\mu_1}\right)\cdot e^{-2\gamma_1 d_1}}{\left(\frac{\gamma_1}{\varsigma}+\frac{\mu_1}{\mu_0}\right)\cdot\left(\frac{\gamma_2}{\gamma_1}+\frac{\mu_2}{\mu_1}\right)+\left(\frac{\gamma_1}{\varsigma}-\frac{\mu_1}{\mu_0}\right)\cdot\left(\frac{\gamma_2}{\gamma_1}-\frac{\mu_2}{\mu_1}\right)\cdot e^{-2\gamma_1 d_1}} \qquad (2)$$

$$k_1=\frac{\sin\left[a_1\xi-b_1\eta+(\xi-\eta)w_1\right]-\sin\left(a_1\xi-b_1\eta\right)}{2(\xi-\eta)}+\frac{\sin\left(a_1\xi+b_1\eta\right)-\sin\left[a_1\xi+b_1\eta+(\xi+\eta)w_1\right]}{2(\xi+\eta)} \qquad (3)$$

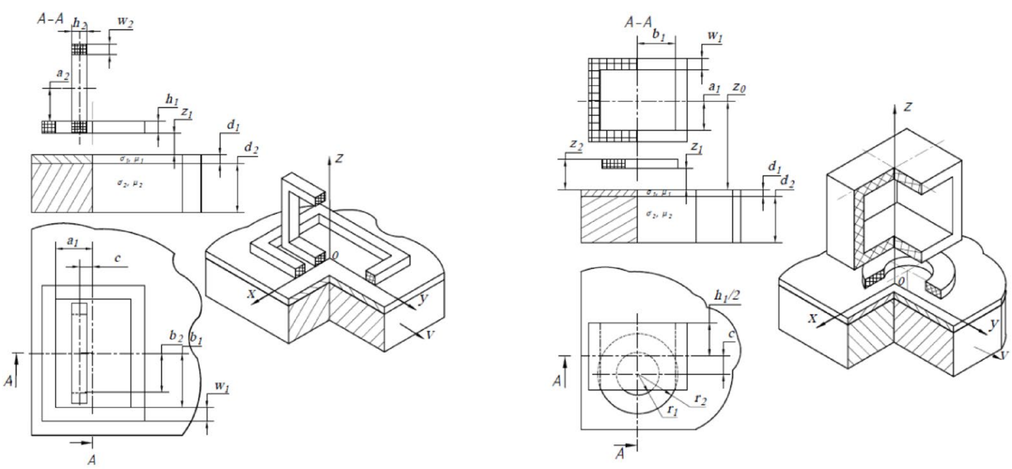

(a) **(b)**

Fig. 1. Variants of self-differential ECP designs for **(a)** probe with rectangular coils and for (**b**) probe with pancake circular pick-up coil.

$$k_2 = \frac{\varsigma \sin\eta\left(b_2+w_2\right)\left[e^{\varsigma(w_2+a_2)}+e^{-\varsigma(w_2+a_2)}\right]-\eta\cos\eta\left(b_2+w_2\right)\left[e^{\varsigma(w_2+a_2)}+e^{-\varsigma(w_2+a_2)}\right]}{\eta^2+\varsigma^2}+ \\ +\frac{\eta\cos\left(\eta b_2\right)\left[e^{\varsigma a_2}-e^{-\varsigma a_2}\right]-\varsigma\sin\left(\eta b_2\right)\left[e^{\varsigma a_2}+e^{-\varsigma a_2}\right]}{\eta^2+\varsigma^2} \quad (4)$$

$$\gamma_1 = \sqrt{\xi^2+\eta^2-j\sigma_1\mu_1\nu\eta+j\omega\sigma_1\mu_1} \quad (5)$$

$$\gamma_2 = \sqrt{\xi^2+\eta^2-j\sigma_2\mu_2\nu\eta+j\omega\sigma_2\mu_2} \quad (6)$$

$$\varsigma = \sqrt{\xi^2+\eta^2} \quad (7)$$

Where ξ and η are Fourier transform integration variables. $\mu_0=4\cdot\pi\cdot10^{-7}$ is the magnetic constant in vacuum. d_1 is the coating thickness. a_1 is the width of the excitation coil. b_1 is the length of the excitation coil. h_1 is the height of the excitation coil cross-section. w_1 is the width of the excitation coil cross-section. a_2 is the width of the pick-up coil. b_2 is the length of the pick-up coil. h_2 is the height of the pick-up coil cross-section. w_2 is the width of the pick-up coil cross-section. c is the axial distance between coils. N_1 is the number of turns in the excitation coil. N_2 is the number of turns in the pick-up coil. μ_1 is the magnetic permeability of the coating. μ_2 is the magnetic permeability of the substrate. σ_1 is the electrical conductivity of the coating. σ_2 is the electrical conductivity of the substrate. v is the speed. z_1 is the lift-off.

And the second one is for tangential multi-turn ECPs with pancake circular pick-up coil and rectangular excitation coil[35]

$$E_c = \frac{-\omega\mu_0 I N_1 N_2}{\pi w_1 h_1\left(r_2-r_1\right)\left(z_2-z_1\right)}\int\limits_{-\infty}^{\infty}\int\limits_{-\infty}^{\infty}\frac{\kappa\hat{k}_1}{\xi\zeta^5}\sin\left(\frac{\eta h_1}{2}\right)e^{-j\eta c_1}\cdot Int\left(r_1\zeta,\ r_2\zeta\right)\cdot\left[e^{-\zeta(z_0+z_1)}-e^{-\zeta(z_0+z_2)}\right]d\xi d\eta \quad (8)$$

In the Eq. (8)

$$Int\left(x_1,x_2\right)=\int\limits_{x_1}^{x_2} xJ_1\left(x\right)dx \quad (9)$$

$$\hat{k}_1 = \left[\frac{\zeta\sin\xi\left(b_1+w_1\right)-\xi\cos\xi\left(b_1+w_1\right)}{\xi^2+\zeta^2}\right]e^{\zeta(a_1+w_1)}-\left[\frac{\zeta\sin\xi b_1-\xi\cos\xi b_1}{\xi^2+\zeta^2}\right]e^{\zeta a_1}+ \\ +\left[\frac{\zeta\sin\xi\left(b_1+w_1\right)+\xi\cos\xi\left(b_1+w_1\right)}{\xi^2+\zeta^2}\right]e^{-\zeta(a_1+w_1)}-\left[\frac{\zeta\sin\xi b_1+\xi\cos\xi b_1}{\xi^2+\zeta^2}\right]e^{-\zeta a_1} \quad (10)$$

Where $J_1()$ is the cylindrical Bessel function of the first kind and first order. r_1 is the inner radius of the cylindrical pick-up coil. r_2 is the outer radius of the cylindrical pick-up coil. z_1 is the lift-off. z_2 is the distance between TO and the upper edge of the cylindrical pick-up coil.

Software products for modelling the measurement process were created based on both of the above mathematical models. To determine their adequacy, test calculations were performed for comparison with the results of experimental and numerical experiments using FEM, which were conducted by the authors of mathematical models and presented in studies[34,35]. For verification calculations, data was used that coincides with that utilized by the authors of the models and is grouped in Tables 1 and 2.

The graphs Fig. 2 obtained show good agreement with those given in articles[34,35]. The functional dependence in Fig. 2a was obtained by calculations using created software from the data in Tables 1 and 2 for comparison with the FEM-modeling results shown in Fig. 5 from[34] for a probe with rectangular coils. The graph in Fig. 2b was constructed for a similar purpose for a probe with a pancake circular pick-up coil. It is intended for comparative analysis with experimental data obtained in Fig. 5 from[35].

Probe with rectangular coils				**Probe with pancake circular pick-up coil**			
excitation coil		**pick-up coil**		**excitation coil**		**pick-up coil**	
a_1 (mm)	12	a_2 (mm)	3	a_1 (mm)	5	r_2 (mm)	9
b_1 (mm)	12	b_2 (mm)	5	b_1 (mm)	12	r_1 (mm)	7.9
z_1 (mm)	1	z_1 (mm)	1	z_0 (mm)	11.9	z_1 (mm)	1.2
w_1 (mm)	2	w_2 (mm)	5	w_1 (mm)	0.5	z_2 (mm)	5.2
h_1 (mm)	8	h_2 (mm)	2	h_1 (mm)	24	c	5
N_1	500	N_2	300	N_1	420	N_2	100
I (A)	1	c (mm)	6	I (A)	0.1		

Table 1. Initial data for verification of software complexes.

Probe with rectangular coils		Probe with pancake circular pick-up coil	
σ_1 (S/m)	$3.8 \cdot 10^7$	σ_1 (S/m)	$3.6 \cdot 10^7$
μ_1	1	μ_1	1
σ_2 (S/m)	$5.8 \cdot 10^7$	σ_2 (S/m)	0
μ_2	1	μ_2	1
d (mm)	0.2	d (mm)	1

Table 2. Parameters of tested objects for verification calculations.

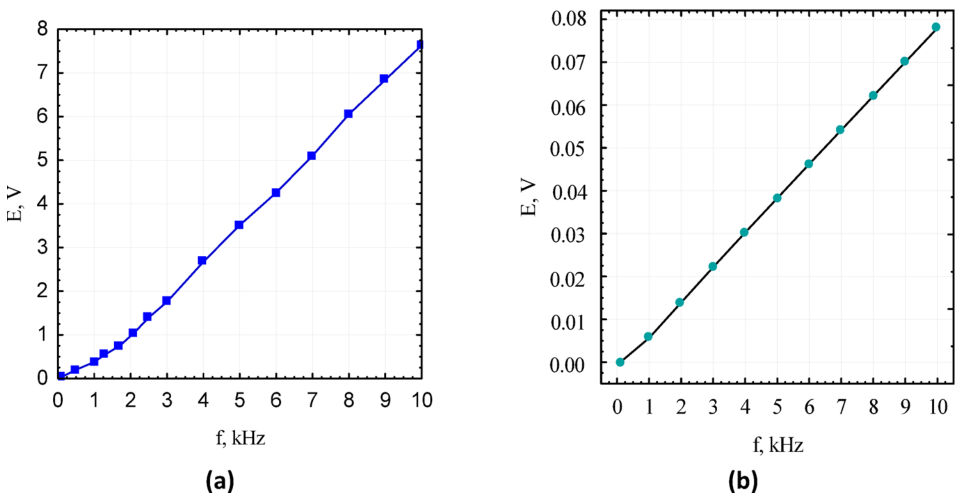

Fig. 2. Results of verification calculations for **(a)** probe with rectangular coils and for **(b)** probe with pancake circular pick-up coil.

Taguchi's robust parameter design methodology for finding optimal designs for meters

Taguchi's robust parametric design method was created for use in quality control engineering and aims to reduce the variability of process or product performance characteristics. In other words, the philosophy of the method is to include quality in the product or process at the design stage[36]. This is achieved by identifying the parameters that have the greatest impact on the quality of the product and finding their design values that will achieve the specified goal and ensure effective operation. The determining factor is that the design process researches the target performance indicator in a specific mixed form of its average value and variance, which Taguchi defined as signal-to-noise ratio. Product design is carried out in such a way that the ratio of signal, i.e., product quality, to noise, i.e., disturbing factors, is maximized. Product quality is observed at randomly selected levels, and those that differ significantly from the average are considered unacceptable.

This approach is ideal for designing ECPs, which are characterized by multi-parameter signals. In different technical applications, some factors may be measurable, while in others, they may be interfering. With this in mind, it is necessary to identify the factors that interfere with measurements, the effect of which on the output signal of the probe must be minimized. For conductivity substrate meters of non-magnetic objects under a conductive coating, these factors include local changes in conductivity and its thickness, as well as lift-off. For weakly magnetic substrates of objects, the heterogeneity of the magnetic permeability of the material, namely its possible variations, is an additional factor. From a physical point of view, these parameter variations are not noise in the classical sense, but represent uncertainties associated with the heterogeneity of the properties of the material of the tested object and the measurement conditions. All these factors are uncontrollable. It should be noted that variations in factors within the Taguchi robust optimization problem in terms of the specified method should be considered as noise components of the signal.

The Taguchi method is experimental because it uses a DOE to determine the influence of design and operating parameters on the output signal of the meter under conditions of noise disturbance caused by the above factors. This design is created using orthogonal arrays, which have special properties. Their distinctive feature is that they check all possible combinations for each pair of parameters, rather than searching through all of them. This leads to a significant reduction in the number of experiments, but the design allows the entire parameter space to be explored. The format of arrays is selected based on the sum of design and operating parameters, which is determined by the design of the meter`s probe, and the level of discretization of these variables accepted in the research. The columns of the DOE are associated with the parameters under research, and the rows correspond to individual experiments. The design is filled in for each experiment with the levels of parameter values.

The selection of possible formats of orthogonal arrays, i.e., L-design, is carried out from reference catalogs listed in specialized literature. The following symbols are used: $L_{NE}(NL^{NP})$, where NE is the number of experiments, NL is the number of levels, and NP is the number of parameters. The number of experiments is calculated according to the equation $NE = (NL - 1) \times NP + 1$. L-design ensures a balance between the number of experiments and the accuracy of the estimation of the impact of all analyzed parameters, a fair comparison of levels for any parameter, and any interaction between them.

Data on the impact of parameters on the SNR of the meter is collected by conducting a series of experiments according to the created DOE. It should be noted separately that the output signals of the ECP are determined by numerical simulation using Eq. (1) or (8) and then used to calculate SNR values, which serve as performance indicators[36]

$$SNR = -10 \cdot \lg\left(Fitness\right) \quad (11)$$

In the Eq. (11)

$$Fitness = \frac{1}{n} \cdot \sum_{i=1}^{n} \frac{1}{\left(\mathrm{mod}\left(E_i\right)\right)^2} \quad (12)$$

Where E_i is the output signal of the probe. n is the sample size.

To implement the optimization algorithm, Taguchi recommends using the Fitness quality loss function, which measures the deviation of the optimized characteristic from the desired target value by mixing the average and variance. The smaller the loss value, the better the match between the obtained value and the desired value. Therefore, a small loss function value leads to a large SNR value. According to Eq. (11), the loss function value is converted to SNR. The type of Fitness function is selected in accordance with the optimization goal. That is, the functional dependence selected for these studies corresponds to the property "larger is better". To find the optimal Taguchi parameters for the substrate conductivity meter, the average $\left(\overline{SNR}\right)$ values are calculated for each parameter and gradation level. Based on the maximum average $\left(\overline{SNR}\right)$ values for different parameters, their optimal combination is determined as a result of associative links with the corresponding gradation levels. Thus, the analysis of main effects is used to optimally combine parameters with the highest average response. This combination of controllable parameters minimizes the influence of noise factors.

After that, a confirmation experiment is performed using a combination of optimal levels. The experiments also include a variance ANOVA-analysis of the data, which allows estimating the relative response value in percent caused by each parameter.

The statistical significance of the parameters is determined using Fisher's test. The design of the experiment ultimately allows for the assessment of complex relationships between parameters. The optimal result obtained using orthogonal arrays is close to that obtained using a full-factor approach. At the same time, parametric design reduces the variations in the output signal of the meter by reducing the influence of the sources of its variation.

Finally, we note that the proposed method for optimal design of meters is rather heuristic. The ECP designs found using this method are locally optimal. There are certain limitations to its application, which are due to the given discrete levels of the analyzed factors. The rather simplified method of representing noise without taking into account its distribution and statistical properties does not allow for an adequate analysis of uncertainty. In addition, the results obtained are only adequate within certain ranges of factor variation, which is characteristic of all studies based on designs of experiments. However, the method also has all the advantages of this approach, as it does not make any assumptions about the functional relationships between influencing factors.

Research on the energy levels of signals from meters with competitive excitation systems

In order to select the best design from two options in terms of output signals, simulations were performed using Eqs. (1) and (8), respectively. At the same time, in order for the results to be considered comparable, the initial data for both design options were set to be as possible identical or measurable. Thus, the following initial parameters were adopted for the excitation coil, as shown in Table 3.

For a rectangular excitation coil, its height above the TO surface is determined by the size z_1 and is 1.5 mm (Fig. 1a). Whereas for a tangential meter, this parameter depends on a number of other design parameters: a_1, w_1, h_2, z_1, and is determined by z_0. Taking into account the distance between the pick-up and excitation coils, $z_0 = 14.5$ mm. The design parameters of the pick-up coils are given in Table 4.

The number of turns in the pick-up coils in both cases is $N_2 = 30$. The operating excitation parameters for both types of meter designs were set as follows: $v = 10$ m/s, $f = 20$ kHz, $I = 0.3$ A. At the same time, for all cases of the tested object structures, the coating thickness d_1 was taken to be 0.3 mm, and the substrate thickness was taken to be infinite. Subsequently, for non-magnetic and weakly magnetic substrate and a series of non-magnetic coatings, the output signals of the designs were determined. In the first experiment, it was assumed

Parameter	a_1 (mm)	b_1 (mm)	h_1 (mm)	w_1 (mm)	N_1
Value	10	16	4.0	1.0	150

Table 3. Design parameters of the excitation coil.

Coil type	Rectangular					Circular			
Parameter	a_2(mm)	b_2(mm)	h_2(mm)	w_2(mm)	c(mm)	r_1(mm)	r_2(mm)	z_1(mm)	z_2(mm)
Value	8.9	8.9	1.0	1.0	2	10.16	11.16	1.5	2.5

Table 4. Design parameters of pick-up coils.

Parameter	Coating material								Substrate material
	Ag	Cu	Au	Mg	Zn	Pt	Cr	Ti	Al
σ (MS/m)	62.1	58.0	45.2	22.0	16.6	9.5	7.9	2.4	36.9

Table 5. Cases of non-magnetic substrate and coating materials.

Probes output signal E	Coating material							
	Ag	Cu	Au	Mg	Zn	Pt	Cr	Ti
ECP with rectangular coils (V)	0.1684	0.1679	0.1661	0.1605	0.1586	0.1556	0.1549	0.1522
Tangential ECP (V)	0.1409	0.1405	0.1389	0.1340	0.1324	0.1297	0.1291	0.1267
Δ (V)	0.0275	0.0274	0.0272	0.0265	0.0262	0.0259	0.0258	0.0254

Table 6. Output signals of probes for object structures with non-magnetic substrate.

Probes output signal E	Coating material							
	Ag	Cu	Au	Mg	Zn	Pt	Cr	Ti
ECP with rectangular coils (V)	0.1695	0.1691	0.1672	0.1064	0.1576	0.1527	0.1514	0.1462
Tangential ECP (V)	0.1418	0.1414	0.1398	0.1338	0.1314	0.1271	0.1260	0.1214
Δ (V)	0.0277	0.0276	0.0274	0.0266	0.0262	0.0256	0.0254	0.0247

Table 7. Output signals of probes for the structure of object with a weakly magnetic substrate.

that the substrate and coating were non-magnetic materials, i.e., their magnetic permeability was μ » 1, and their electrical conductivities are given in Table 5. Accordingly, for the second experiment, a weakly magnetic material, monickel (Ni + Cu), was selected as the substrate, for which the electrophysical parameters are as follows: $\sigma = 60$ MS/m, $\mu = 4.1$, and the coating options were specified as in the previous case.

The output signal E for both designs of eddy current probes for the first experiment, when the substrate material is non-magnetic, is shown in Table 6, and for the second experiment, in Table 7. In addition, for comparison of the designs, Tables 6 and 7 show the difference in signal levels Δ.

Thus, the results obtained indicate a slight difference in signals of approximately 25 mV for ECP designs with rectangular coils and their tangential variant. That is, there is no absolute and significant advantage in the energy level of the signal of one design over another, and it is difficult to choose the best one. Therefore, in the future, we will study and analyze the ability of both of these designs to provide the maximum SNR value, which will be considered the selection criterion.

Taguchi's design of experiments for rectangular coils meters

First, let us consider the construction of Taguchi's design of experiments for eddy current probe with rectangular coils (Fig. 1a) in two cases of substrate: the first is a non-magnetic substrate and coating, and the second is a weakly magnetic substrate and non-magnetic coating. The prerequisite for choosing one or another orthogonal array, on the basis of which Taguchi's design of experiments is based, is to establish the number of design and operating parameters for the selected probe design. Thus, for the ECP design with rectangular coils, the design parameters are: length, width, height, and cross-sectional width of the excitation coil; length, width, height, and cross-sectional width of the pick-up coil and the center-to-center distance between the coils, and the operating parameters are the frequency of the electromagnetic field and the speed of movement of the TO. Thus, the total number of these parameters is $NP = 11$, which makes it possible to determine the format of the orthogonal array $L_{50}(2^1, 5^{11})$[37], which requires $NE = 50$ experiments and $NL = 2$ gradation levels for one factor and $NL = 5$ for eleven. The properties of orthogonal arrays allow us to remove excess factors and use only the necessary number of them[36]. Then, from this orthogonal array, we do not use factor 2^1, which gives a rather rough its gradation on only two levels. Therefore, we finally use a modified orthogonal array $L_{50}(5^{11})$, which completely covers the needs in terms of the number of factors and has an increased discretization for each factor.

To create a Taguchi design of experiments for this array, ECP parameters were set in the following ranges: $a_1 = 10–22$ mm, $b_1 = 16–28$ mm, $h_1 = 4–8$ mm, $w_1 = 1–4$ mm, $a_2 = 8–14$ mm, $b_2 = 8–14$ mm, $h_2 = 1–2$ mm,

$w_2 = 1–4$ mm, $c = 2–8$ mm, $f = 20–30$ kHz, $v = 10–25$ m/s. The excitation current was constant and equal to $I = 0.3$ A.

The implementation of Taguchi's design of experiments involves determining the output signals of the meter under noise disturbances, which are also formed by an orthogonal array. Therefore, we also apply the $L_{50}(2^1, 5^{11})$ array with its modifications. In the case of a non-magnetic substrate, when there are three noise factors, we use $L_{50}(5^3)$, and for a weakly magnetic substrate, we use $L_{50}(5^4)$. At the same time, noise factors, which are the same for both non-magnetic and weakly magnetic substrates, were set in the following ranges: $d = 0.3–1.3$ mm, $z_1 = 1.5–2.5$ mm. Two types of object structures with two different coating and substrate materials were studied. The electrophysical properties of a non-magnetic aluminum substrate with a chrome coating were taken as follows: σ_1 = (6.32–9.47) MS/m, $\sigma_2 = 36.9$ MS/m.

For the object with a weakly magnetic substrate and a titanium coating, these properties were as follows: $\mu_2 = 3.28–4.91$, σ_1 = (1.92–2.88) MS/m, $\sigma_2 = 60$ MS/m. The final DOE for eleven design and operating parameters is shown in Table 8. The same table shows the results of calculating the output signal of the ECP with rectangular coils under the influence of noise factors with their 50 combinations, which are given in Table 9 for a non-magnetic substrate and Table 10 for a weakly magnetic one. The numerical values in the numerator correspond to case 1 of the substrate, and those in the denominator correspond to case 2. The results obtained for both analyzed substrate examples are then used to calculate the *SNR* values (Table 8).

Taguchi's design of experiments for tangential meters

When constructing a DOE for this type of design, we focus only on the differences inherent in it (Fig. 1b). That is, the design parameters of a circular coil are its outer and inner radii, and all other parameters are the same as previous case. Their total number is $NP = 10$. Therefore, to create a design of experiments, we use the orthogonal array $L_{50}(2^1, 5^{11})$ with its modification $L_{50}(5^{10})$ using the same initial data as above. The outer and inner radii of

№	Controllable parameters								Output signal (V)					SNR (dB)
	a_1 (mm)	b_1 (mm)	h_1 (mm)	…	w_2 (mm)	c (mm)	f (kHz)	v (m/s)	1	2	…	49	50	
1	10	16	4	…	1.00	2.0	20.0	10.00	0.1072	0.1009	…	0.0845	0.0803	−20.86
									0.1030	0.0964	…	0.0743	0.0706	−21.61
2	10	19	5	…	1.25	3.5	22.5	13.75	0.2560	0.2418	…	0.2062	0.1965	−13.17
									0.2470	0.2311	…	0.1829	0.1740	−13.88
3	10	22	6	…	1.50	5.0	25.0	17.50	0.4600	0.4360	…	0.3776	0.3606	−7.97
									0.4454	0.4203	…	0.3378	0.3221	−8.63
4	10	25	7	…	1.75	6.5	27.5	21.25	0.7024	0.6669	…	0.5827	0.5571	−4.24
									0.6815	0.6443	…	0.5238	0.5001	−4.86
5	10	28	8	…	2.00	8.0	30.0	25.00	1.0152	0.9679	…	0.8581	0.8230	−0.92
									0.9881	0.9386	…	0.7790	0.7464	−1.49
…	…	…	…	…	…	…	…	…	…	…	…	…	…	…
20	19	28	6	…	1.25	8.0	25.0	10.00	0.6596	0.6309	…	0.5597	0.5386	−4.63
									0.6422	0.6119	…	0.5099	0.4901	−5.17
21	22	16	8	…	1.5	3.5	20.0	25.00	0.1375	0.1324	…	0.1189	0.1152	−18.11
									0.1343	0.1289	…	0.1098	0.1062	−18.57
22	22	19	4	…	1.75	5.0	22.5	10.00	0.3090	0.2987	…	0.2717	0.2637	−10.98
									0.3027	0.2916	…	0.2524	0.2446	−11.41
23	22	22	5	…	2.00	6.5	25.0	13.75	0.5693	0.5483	…	0.4957	0.4798	−5.74
									0.5567	0.5345	…	0.4581	0.4427	−6.20
24	22	25	6	…	1.00	8.0	27.5	17.50	0.6368	0.6137	…	0.5574	0.5395	−4.74
									0.6233	0.5989	…	0.5160	0.4987	−5.19
…	…	…	…	…	…	…	…	…	…	…	…	…	…	…
46	22	16	8	…	1.75	6.5	25.0	10.00	0.4179	0.4019	…	0.3620	0.3499	−8.46
									0.4083	0.3914	…	0.3334	0.3218	−8.94
47	22	19	4	…	2.00	8.0	27.5	13.75	0.4717	0.4542	…	0.4119	0.3984	−7.37
									0.4615	0.4431	…	0.3808	0.3678	−7.82
48	22	22	5	…	1.00	2.0	30.0	17.50	0.1518	0.1468	…	0.1349	0.1308	−17.11
									0.1490	0.1437	…	0.1258	0.1218	−17.51
49	22	25	6	…	1.25	3.5	20.0	21.25	0.1933	0.1872	…	0.1704	0.1656	−15.03
									0.1894	0.1828	…	0.1587	0.1541	−15.44
50	22	28	7	…	1.50	5.0	22.5	25.00	0.3159	0.3051	…	0.2767	0.2684	−10.82
									0.3092	0.2976	…	0.2566	0.2486	−11.25

Table 8. DOEs for the ECP design with rectangular coils.

№	Parameter`s values											
	1	2	3	…	30	31	32	33	…	48	49	50
d (mm)	0.30	0.30	0.3	…	0.30	0.55	0.55	0.55	…	1.3	1.30	1.30
z_1 (mm)	1.50	1.75	2.0	…	2.50	1.50	1.75	2.00	…	2.00	2.25	2.50
σ_1 (MS/m)	6.32	7.11	7.9	…	9.47	7.11	7.90	8.69	…	7.11	7.90	8.69

Table 9. Design of experiments for noise factors for non-magnetic substrate.

№	Parameter`s values											
	1	2	3	…	30	31	32	33	…	48	49	50
d (mm)	0.30	0.30	0.30	…	0.30	0.55	0.55	0.55	…	1.3	1.30	1.30
z_1 (mm)	1.50	1.75	2.00	…	2.50	1.50	1.75	2.00	…	2.00	2.25	2.50
σ_1 (MS/m)	1.92	2.16	2.40	…	2.88	2.16	2.40	2.64	…	2.16	2.40	2.64
μ_2	3.28	3.69	4.10	…	4.10	3.28	3.69	4.10	…	4.50	4.91	3.28

Table 10. Design of experiments for noise factors for weakly magnetic substrate.

the pick-up coil were accepted in the range: $r_1 = 10.16–12$ mm, $r_2 = 12.5–18$ mm. For this type of design, Table 11 shows the DOE for ten design and operating parameters with fifty experiments. The result according to this design of experiments was obtained at similar values of noise factors, which are given in Tables 9 and 10.

Comparative analysis based on the *SNR* criterion of optimal designs for conductivity meters

Based on the obtained *SNR* values (Tables 8 and 11), the optimal Taguchi parameters are searched. Specifically, *SNR* grouping is performed in advance for each parameter and gradation level, and their average values are calculated. Based on the associative relationships between the maximum values of the average $\left(\overline{SNR}\right)$ for different parameters and the corresponding levels of their gradations, an optimal set is formed for the first structure of the meter and the object with a non-magnetic substrate, as shown in Fig. 3. For the same meter in the case of a weakly magnetic substrate, a similar optimal design is obtained.

The following optimal parameters were obtained for the tangential meter (Table 12). It should be noted that the parameters are the same for both non-magnetic and weakly magnetic substrates.

Confirmatory experiment to establish the optimality of the meter design

Confirmatory experiments were also conducted to determine the *SNR* values that provide the optimal designs obtained for both substrate options. That is, with the same variations in the influence of uncontrollable noise parameters, the EMF values and the *SNR* were determined. The obtained *SNR* values for the considered types of optimal designs with different substrate options are shown in Fig. 4. To verify that non-optimized designs have lower *SNR* values, Figs. 5 and 6 show their values for all 50 options.

Thus, the obtained *SNR* values indicate that the best level is provided by the probe structure with rectangular coils for both materials TO structures. Therefore, this particular variant of the optimal probe design was considered in further studies.

Variance ANOVA-analysis of the influence of meter parameters on *SNR*

Subsequently, for the selected ECP with rectangular coils, a multifactor variance ANOVA-analysis was performed using Fisher's criterion[38,39] to assess the influence of design parameters on *SNR*. At the same time, a preliminary check of the prerequisites for the application of ANOVA-analysis was performed, the fulfillment of which gives grounds for its adequate use. As a result, a number of statistical indicators were obtained for all design and operating parameters of this probe design with different substrate options. Thus, for a non-magnetic substrate, the results are given in Table 13, and for a weakly magnetic substrate, in Table 14, where the following designations are used: *SS* – sum of squares of the variance component and residuals, *MS* – mean square of the variance component and residuals, *F* is the variation ratio at a given degree of freedom equal to 4, *p* is the probability of a random effect of a factor on the resultant feature, and *W* is the contribution of each factor to the total its effect (%).

Then, the statistical significance of each factor is established by checking the condition $F > F_{\alpha,t_1,t_2}$, where $\alpha = 5\%$ is the accepted significance level, t_1 is the number of degrees of freedom of the corresponding factor, t_2 is the number of degrees of freedom of all random factors, F_{α,t_1,t_2} is the critical value of Fisher's criterion (for this study it is 3.48). Thus, for both cases of substrate materials, the statistical insignificance of the same parameters of the probes, such as the width of the excitation coil w_1, the height h_2 and the width w_2 of the pick-up coil, and the speed of movement of the tested object v, is observed. At the same time, the most influential design parameter is the center-to-center distance between the coils, which accounts for 74% of the total influence of all factors.

№	Controllable parameters								Output signal (V)					SNR (dB)
	w_1 (mm)	r_1 (mm)	r_2 (mm)	…	h_2 (mm)	c (mm)	f (kHz)	v (m/s)	1	2	…	49	50	
1	1.00	10.16	12.50	…	1.00	2.0	20.0	10.00	0.1363	0.1269	…	0.1033	0.0974	−19.02
									0.1365	0.1269	…	0.0891	0.0838	−19.67
2	1.75	10.62	13.87	…	1.25	3.5	22.5	13.75	0.2732	0.2558	…	0.2132	0.2018	−12.81
									0.2733	0.2555	…	0.1852	0.1751	−13.44
3	2.50	11.08	15.25	…	1.50	5.0	25.0	17.50	0.4270	0.4019	…	0.3418	0.3247	−8.78
									0.4267	0.4009	…	0.2995	0.2846	−9.37
4	3.25	11.54	16.62	…	2.00	6.5	27.5	21.25	0.5890	0.5572	…	0.4824	0.4599	−5.85
									0.5881	0.5554	…	0.4267	0.4072	−6.40
5	4.00	12.00	18.00	…	1.00	8.0	30.0	25.00	0.7542	0.7168	…	0.6305	0.6031	−3.57
									0.7526	0.7142	…	0.5630	0.5395	−4.09
…	…	…	…	…	…	…	…	…	…	…	…	…	…	…
20	1.00	11.54	13.87	…	1.75	3.5	30.0	17.50	0.4332	0.4084	…	0.3522	0.3347	−8.57
									0.4321	0.4068	…	0.3097	0.2949	−9.17
21	3.25	11.08	13.87	…	1.75	5.0	22.5	10.00	0.3208	0.3017	…	0.2546	0.2419	−11.31
									0.3209	0.3013	…	0.2231	0.2118	−11.89
22	4.00	11.54	15.25	…	2.00	6.5	25.0	13.50	0.4892	0.4622	…	0.3970	0.3784	−7.51
									0.4888	0.4611	…	0.3506	0.3342	−8.07
23	1.00	12.00	16.25	…	1.00	8.0	27.5	17.50	0.9528	0.9003	…	0.7776	0.7407	−1.69
									0.9513	0.8975	…	0.6860	0.6542	−2.26
24	1.75	10.16	18.00	…	1.25	2.0	30.0	21.25	0.2808	0.2656	…	0.2295	0.2184	−12.30
									0.2802	0.2642	…	0.2029	0.1936	−12.87
…	…	…	…	…	…	…	…	…	…	…	…	…	…	…
46	1.75	10.62	18.00	…	1.50	6.5	27.5	17.50	0.5967	0.5633	…	0.4852	0.4618	−5.78
									0.5958	0.5615	…	0.4273	0.4071	−6.36
47	2.50	11.08	12.50	…	1.75	8.0	30.0	21.25	0.6665	0.6279	…	0.5404	0.5132	−4.85
									0.6648	0.6252	…	0.4737	0.4508	−5.46
48	3.25	11.54	13.87	…	2.00	2.0	20.0	25.00	0.1357	0.1279	…	0.1077	0.1025	−18.76
									0.1359	0.1279	…	0.0955	0.0907	−19.28
49	4.00	12.00	15.25	…	1.00	3.5	22.5	10.00	0.3335	0.3150	…	0.2689	0.2564	−10.87
									0.3336	0.3146	…	0.2378	0.2266	−11.41
50	1.00	10.16	16.62	…	1.25	5.0	25.0	13.75	0.5629	0.5319	…	0.4569	0.4355	−6.29
									0.5625	0.5307	…	0.4036	0.3847	−6.84

Table 11. DOEs for the design of a tangential ECP.

Numerical-experimental research of signal variability in meters using the Monte-Carlo method

In the following experiments, we will use the Monte-Carlo method to prove the effectiveness of suppressing noise parameters that cause variations in the output signal of the probe around the undistorted case.

Therefore, according to the algorithm of this method, we will sequentially generate noise parameters in the ranges specified in Tables 9 and 10, and during the simulation of measurements, we will observe changes in the ECP signal, whose designs are optimal for non-magnetic and weakly magnetic substrates caused by these interferences. In addition, parameters for noise modelling were generated at predetermined intervals in accordance with the law of uniform distribution to ensure equal probability of their values occurring. The number of implementations in the series was 30, although it could be arbitrarily large, but it is important to choose a number that makes it impossible for the noise parameters to coincide with those shown in Tables 9 and 10. Comparison with the results of similar observations for the best (worst) non-optimal design options in terms of *SNR* (Tables 8 and 11) allows us to verify the effectiveness of the designs found in terms of reducing signal variance.

For the case when the substrate is non-magnetic, four numerical experiments were carried out, in each of which the noise factor, the influence of which was investigated, varied, while other noise parameters were fixed. Thus, in the first experiment, the noise parameter was the lift-off z_1, while the other parameters were set as follows: $d = 0.3$ mm, $\mu_1 = \mu_2 = 1$, $\sigma_1 = 7.9$ MS/m, $\sigma_2 = 36.9$ MS/m. In the second experiment, $d = \text{var}$, $z_1 = 1.5$ mm, and the other parameters were taken from the previous experiment. In the third experiment, the noise parameter is the electrical conductivity of the coating material $\sigma_1 = \text{var}$, and all other parameters are constant. In the last experiment, the influence of three noise parameters z_1, d, σ_1 was studied simultaneously. Thus, Table 15 groups the initial data on noise parameters at which these numerical experiments were performed.

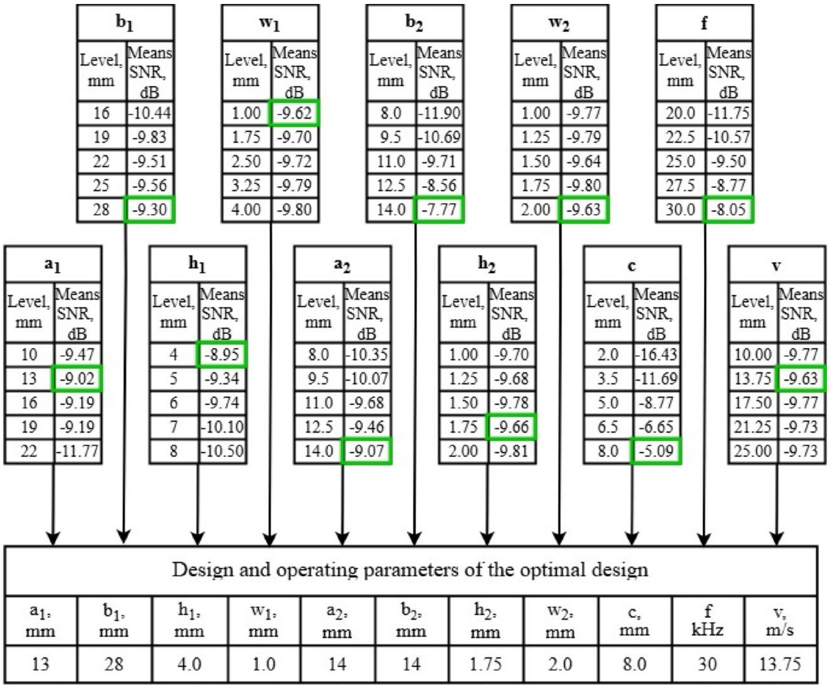

Fig. 3. Determination of optimal parameters for a meter with rectangular coils and a non-magnetic substrate.

Taguchi-parameters	a_1 (mm)	b_1 (mm)	h_1 (mm)	w_1 (mm)	a_2 (mm)	b_2 (mm)	h_2 (mm)	c (mm)	f (kHz)	v (m/s)
Values	22	28	4.0	1.0	12	18	1.0	8.0	30	10

Table 12. Parameters of the optimal design of a tangential ECP.

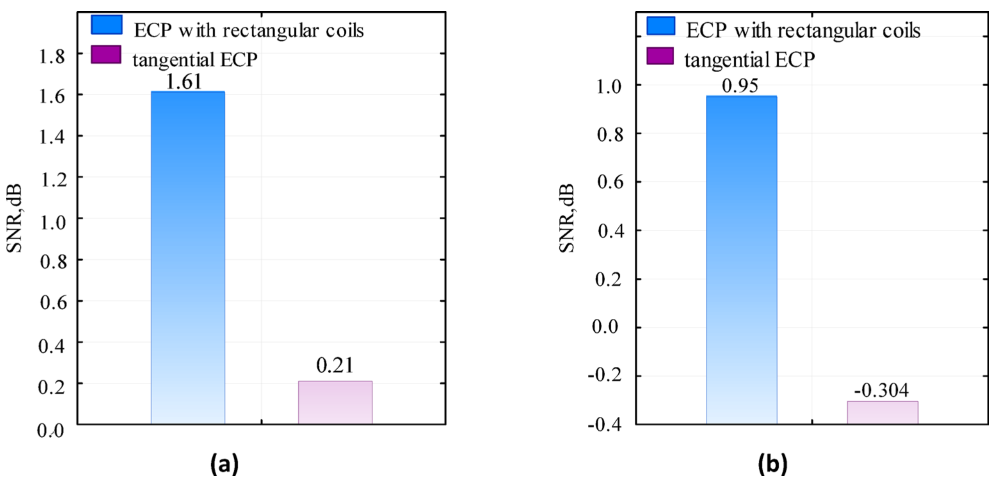

Fig. 4 . *SNR* values of optimal designs **(a)** for non-magnetic substrate material and **(b)** for weakly magnetic substrate.

The obtained dependencies of the relative deviation δ, % of the output signals of the ECP from the change in the lift-off z_1 of the optimized and two variants of non-optimized designs are shown in Fig. 7, the coating thickness d – in Fig. 8, the electrical conductivity of the coating material σ_1 – in Fig. 9. The case of their combined simultaneous action is demonstrated in Fig. 10.

For the optimal design, the relative error under the influence of lift-off is in the range from 0.042% to 16.35%, and the best option of the non-optimized design provides this indicator from 0.044% to 16.56%, while the worst option has a range of 0.086–21.34%. When coating thickness was taken as the noise factor, the ranges of relative

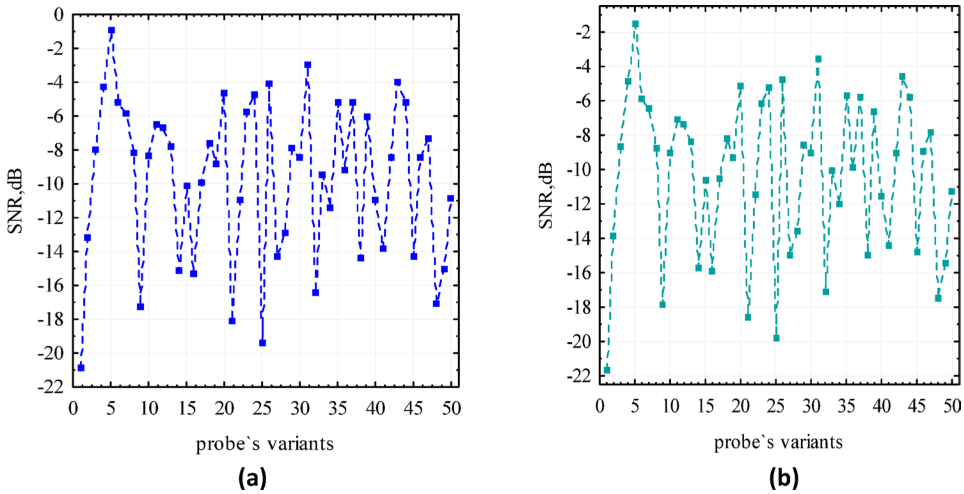

Fig. 5. *SNR* values for non-optimized designs of ECPs with rectangular coils for **(a)** non-magnetic substrate and for **(b)** weakly magnetic substrate.

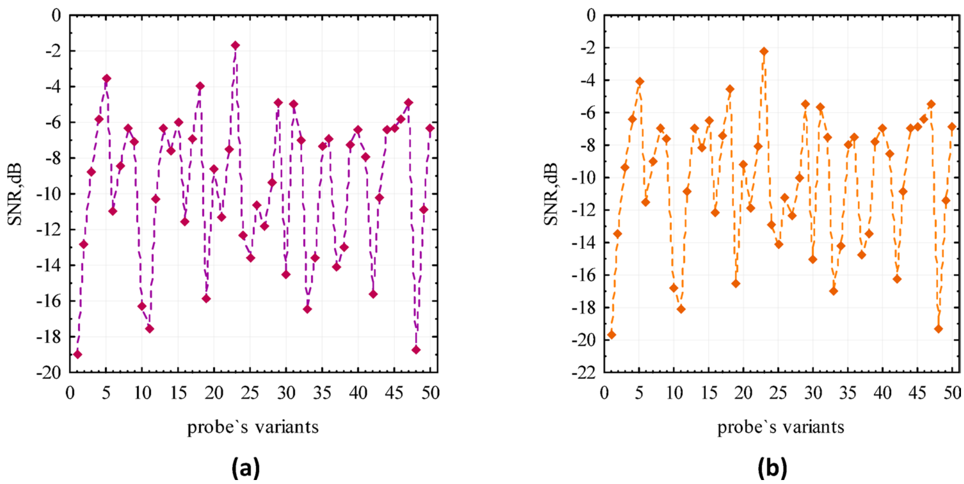

Fig. 6. *SNR* values for non-optimized designs of tangential ECPs for **(a)** case of non-magnetic substrate and **(b)** case of weakly magnetic substrate.

Parameters	SS	MS	F	*p*	W %
a_1	53.3742	13.3436	590.496	0.0000010	4.90
b_1	7.7065	1.9266	85.260	0.0000870	0.70
h_1	14.8633	3.7158	164.437	0.0000170	1.36
w_1	0.1934	0.0483	2.140	0.2129190	0.01
a_2	10.0843	2.5211	111.566	0.0000450	0.92
b_2	108.7111	27.1778	1202.705	0.0000001	9.99
h_2	0.1597	0.0399	1.766	0.2723730	0.01
w_2	0.2850	0.0713	3.154	0.1197910	0.02
c	806.8092	201.7023	8925.985	0.0000001	74.16
f	85.6087	21.4022	947.116	0.0000001	7.86
v	0.1232	0.0308	1.364	0.3645390	0.01
residual	0.113	0.0226			

Table 13. Results of ANOVA-analysis for the probe in determining the electrical conductivity of a non-magnetic substrate.

Parameters	SS	MS	F	*p*	W %
a_1	46.6011	11.6503	548.615	0.0000010	4.29
b_1	8.6689	2.1672	102.055	0.0000560	0.79
h_1	14.6468	3.6617	172.431	0.0000150	1.35
w_1	0.1190	0.0297	1.401	0.3544060	0.01
a_2	10.3954	2.5989	122.381	0.0000360	0.95
b_2	108.6785	27.1696	1279.425	0.0000001	10.02
h_2	0.1524	0.0381	1.794	0.2672380	0.01
w_2	0.2745	0.0686	3.232	0.1151350	0.02
c	808.2808	202.0702	9515.540	0.0000001	74.52
f	86.6142	21.6535	1019.671	0.0000001	7.98
v	0.1135	0.0284	1.336	0.3722980	0.01
residual	0.1062	0.0212			

Table 14. Results of ANOVA-analysis for the probe in determining the electrical conductivity of a weakly magnetic substrate.

	Experiment 1	Experiment 2	Experiment 3	Experiment 4		
№	z_1 (mm)	d (mm)	σ_1 (MS/m)	z_1 (mm)	d (mm)	σ_1 (MS/m)
1	2.03	0.97	7.592	2.13	0.30	8.469
2	2.34	0.62	6.753	1.55	0.41	7.496
3	2.16	0.61	6.529	1.76	0.61	6.478
4	2.34	0.41	8.132	2.40	0.34	6.856
5	1.61	1.1	8.052	2.23	0.49	7.301
…	…	…	…	…	…	…
26	1.69	0.79	8.512	2.16	0.89	8.119
27	1.68	0.80	7.139	1.60	1.25	8.446
28	1.96	0.81	7.981	1.55	0.69	6.352
29	1.60	0.99	7.580	1.96	0.49	7.399
30	1.60	0.91	8.170	2.23	0.87	8.756

Table 15. Noise factors for the case of a non-magnetic substrate.

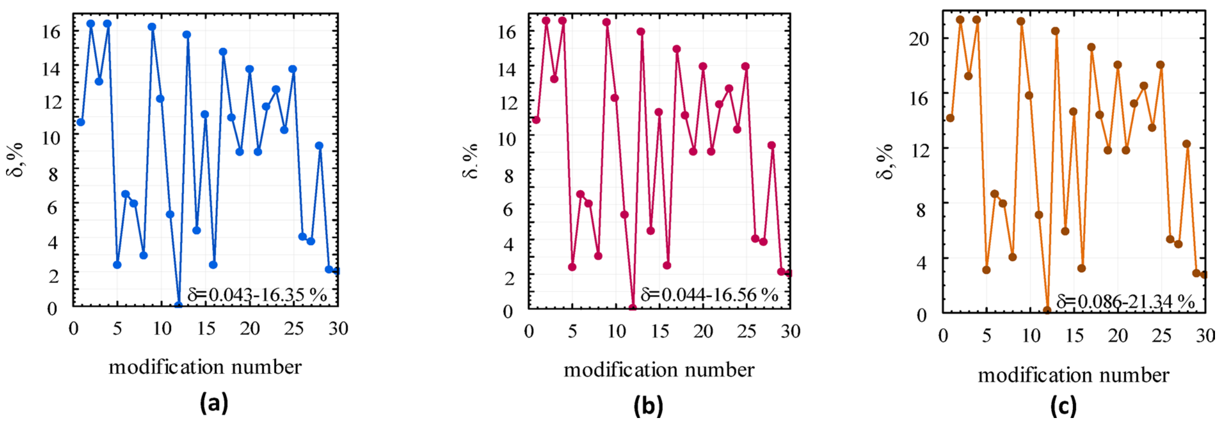

Fig. 7. Dependences of the absolute value of the relative deviation δ, % of the output signals of the ECP on variations of lift-off z_1 **(a)** for the optimized design, **(b)** for the best non-optimized design, **(c)** for the worst non-optimized design.

deviation variation for the designs under consideration (Fig. 8) were as follows: for the first – 0.8–3.22%, for the second – 0.82–3.29%, and for the third – 1.19–6.33%. The smallest variations are observed when the electrical conductivity of the coating material was taken as the interfering factor (Fig. 9). Thus, for the optimal design, these variations in relative error range from 0.018% to 0.35%, while for the best option of a non-optimal design, they range from 0.019% to 0.36%, and the worst option has 0.024–0.45%. With the simultaneous combined

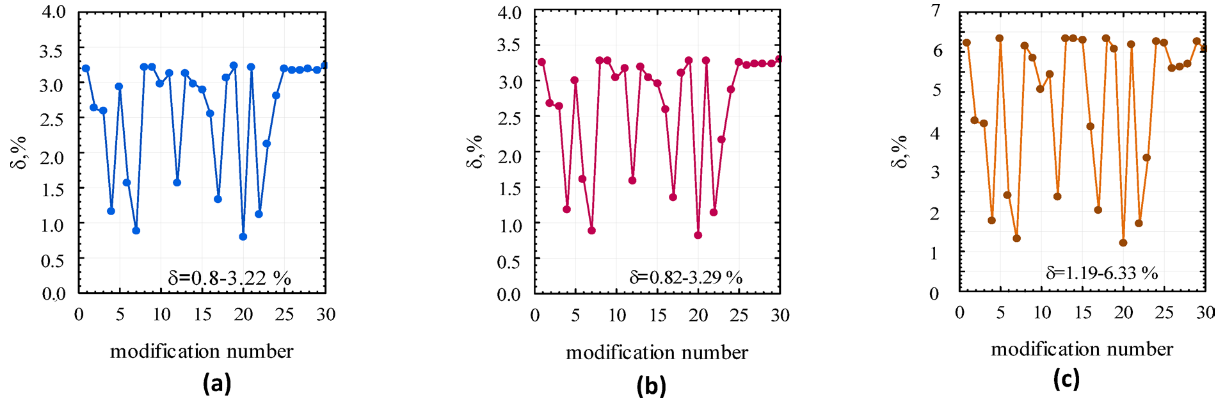

Fig. 8. Dependences of the absolute value of the relative deviation δ, % of the output signals of the ECP on variations of d(**a**) for the optimized design, (**b**) for the best non-optimized design, (**c**) for the worst non-optimized design.

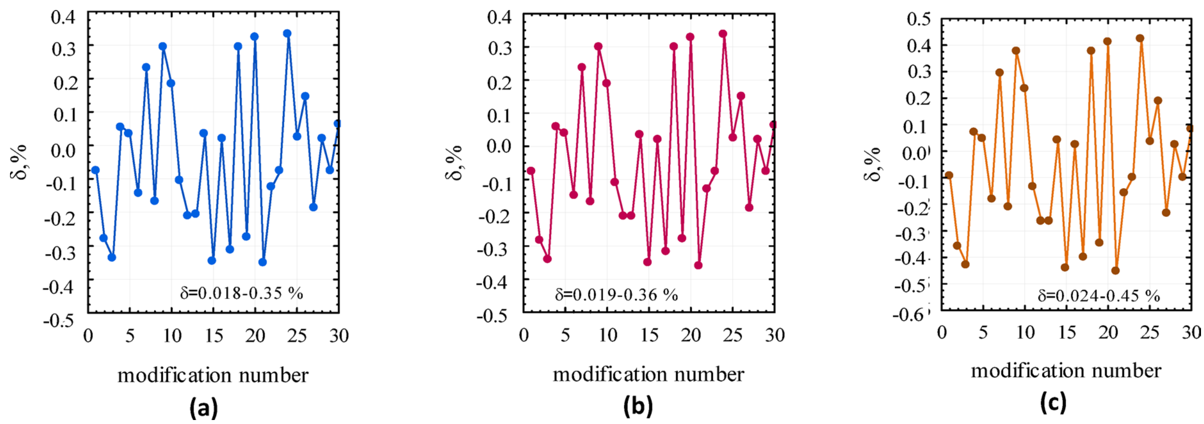

Fig. 9. Dependencies of the relative deviation δ, % of the output signals of the ECP on variations of σ_1(**a**) for the optimized design, (**b**) for the best non-optimized design, (**c**) for the worst non-optimized design.

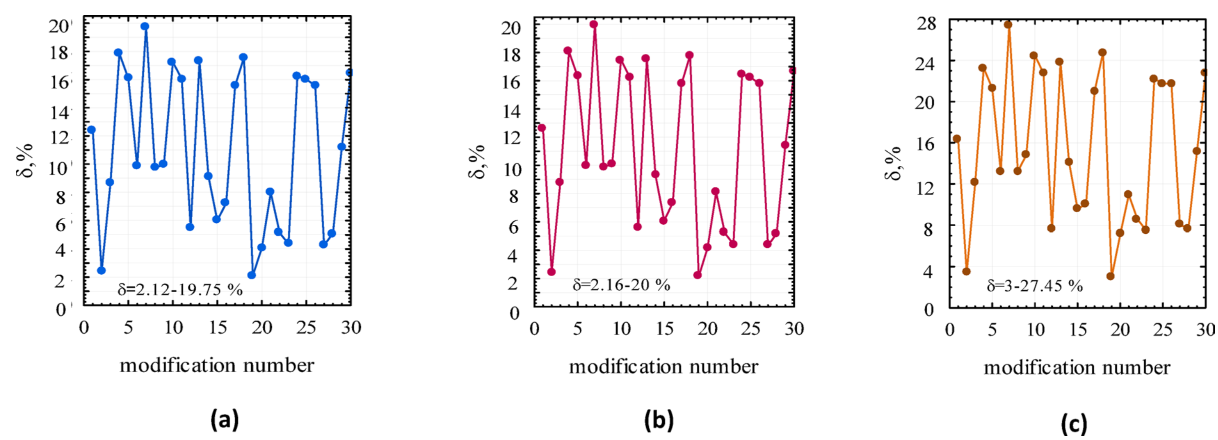

Fig. 10. Dependences of the absolute value of the relative deviation δ, % of the output signals of the ECP from z_1, d, σ_1(**a**) for the optimized design, (**b**) for the best non-optimized design, (**c**) for the worst non-optimized design.

	Experiment 1	Experiment 2	Experiment 3	Experiment 4	Experiment 5			
№	z_1 (mm)	d (mm)	σ_1 (MS/m)	μ_2	z_1 (mm)	d (mm)	σ_1 (MS/m)	μ_2
1	2.14	0.54	2.520	3.87	1.66	0.35	2.62	4.41
2	1.92	0.95	2.536	3.66	2.29	0.30	2.56	4.15
3	1.59	0.32	2.454	3.66	1.94	1.06	2.70	3.51
4	2.20	0.44	2.348	4.17	2.01	0.41	2.88	4.47
5	2.16	0.85	2.876	3.37	1.57	0.97	2.12	3.33
…	…	…	…	…	…	…	…	…
26	1.55	0.81	2.819	3.65	2.10	0.85	2.60	3.53
27	1.60	0.75	2.078	3.29	1.69	1.30	2.62	4.73
28	2.15	1.24	2.032	3.42	1.73	1.17	2.80	3.60
29	2.41	0.55	2.034	4.68	1.74	0.48	2.69	4.34
30	1.93	1.03	2.477	4.61	1.91	0.58	2.30	4.77

Table 16. Noise factors for the case of a weakly magnetic substrate.

influence of all the noise factors mentioned here, we have the following relative deviations, whose values range from 2.12% to 19.75% for the optimized design option, from 2.16% to 20.00% for the best non-optimized design option, and from 2.99% to 27.45% for the worst non-optimized design option.

A similar study was conducted when analyzing TO with a weakly magnetic substrate. However, in this case, another noise factor is added - the magnetic permeability of the substrate. Table 16 shows some numerical values of noise parameters for performing experiments.

The parameters and electrophysical properties of the materials were taken as follows: $d = 0.3$ mm, $\mu_1 = 1$, $\sigma_1 = 2.4$ MS/m, $\sigma_2 = 60$ MS/m, $\mu_2 = 4.1$ – experiment 1; $z_1 = 1.5$ mm, $\mu_1 = 1$, $\sigma_1 = 2.4$ MS/m, $\sigma_2 = 60$ MS/m, $\mu_2 = 4.1$– experiment 2; $d = 0.3$ mm, $z_1 = 1.5$ mm, $\mu_1 = 1$, $\sigma_2 = 60$ MS/m – experiment 3; $d = 0.3$ mm, $\mu_1 = 1$, $\sigma_1 = 2.4$ MS/m, $\sigma_2 = 60$ MS/m – experiment 4; $\mu_1 = 1$, $\sigma_2 = 60$ MS/m – experiment 5.

Thus, these experiments also show a reduction in output signal variations for the optimized design compared to the non-optimized ones. In the first experiment, the maximum relative deviation is 17.49%, 17.7%, and 22.75% for the specified design options. For the second experiment, these indicators are as follows: 9.27%, 9.42%, and 14.3%. When the noise factor is the electrical conductivity of the coating material, a slight variation in output signals is obtained with a relative deviation ranging from 0.0011% to 0.326% for the optimized design, and slightly higher values for the non-optimized designs. Variations in the magnetic permeability of the substrate material also produce insignificant signal fluctuations with relative deviations in the range of 0.028–0.63% and higher values for non-optimized designs, ranging from 0.64% to 1.12%. With the simultaneous cumulative effect of all four noise factors, the range of relative deviation when using the optimal probe design is from 2.67% to 22.76% and, accordingly, 3.53–30.5% for the non-optimized design.

Conclusions

In summary, it should be noted that in this study, for movable surface self-differential eddy current conductivity meters of non-magnetic and weakly magnetic substrates of an object located under a layer of metal coating, a method of suppressing all noises characteristic of this problem was implemented based on Taguchi optimization. As a simulation result, two optimal designs were obtained for the tangential type and with rectangular coil meters, which turned out to be the same for measurements of the conductivity of TO with non-magnetic and weakly magnetic substrates. It was established that the optimal design of the ECP with rectangular coils in the case of a non-magnetic substrate of the TO has a signal-to-noise ratio of 1.61 dB, while the best of the non-optimized designs has a negative *SNR* of 0.92 dB, and the worst also has a negative *SNR* of 20.86 dB. At the same time, even if we consider the minimum *SNR* increase of 2.53 dB from these options, this gives an increase in the meter signal level of approximately 25.8%. Similar results were obtained for the measurement of the electrical conductivity of a weakly magnetic TO. A confirmatory experiment established that the best *SNR* level is provided by a probe structure with rectangular coils. Thus, for measurements on a non-magnetic substrate, this design has an *SNR* value 7.6 times higher, and in tests on a weakly-magnetic TO in 4 times higher compared to the tangential design of the meter.

Numerical-experimental Monte Carlo experiments have shown that signal variations, estimated by relative deviations for both substrate cases, are approximately of the same order of magnitude. It should also be noted that in all cases, the optimized design of the meter provides smaller signal variations. Thus, assuming that only noise factor z_1 is present, the maximum relative signal deviation for this design is almost 5% less than for the worst non-optimized version. This indicator is slightly lower, by 3%, when the noise factor is the coating thickness. The maximum relative deviation of 0.35% for the optimal design and 0.45% for the non-optimized design was quite insignificant when only the influence of the variation in electrical conductivity of the coating material was taken into account. In this case, the deviation indicator improved by only 0.1%. A reduction in relative deviation of almost 7.7% is observed when the signals to the meter are obtained taking into account the simultaneous action of all noise factors. Thus, in all numerical experiments, there is a more or less decrease in the relative deviation for the optimized design option, which indicates its effectiveness compared to the non-optimized options.

Using ANOVA variance analysis based on its statistical indicators, the significance of the design and operating parameters of the eddy current meter was determined. Thus, for both TO substrate materials, the same number of statistically insignificant probe parameters were identified, namely the width of the excitation coil w_1 and height h_2, the width of the pick-up coil w_2, and the speed of movement of the tested object v. Then, the variation ranges of design parameters in order of decreasing its influence is as follows: the center-to-center distance between the coils, the length of the pick-up coil, the excitation frequency, the width and height of the excitation coil cross-section, the width of the pick-up coil, and the length of the excitation coil.

Data availability

The datasets used in this study are publicly available and subject to their respective licensing terms. The UCI HAR dataset is available at: https://www.kaggle.com/c/uci-har and is distributed under the Creative Commons Attribution 4.0 International (CC BY 4.0) license, permitting sharing and adaptation with proper citation. The PAMAP2 Physical Activity Monitoring dataset is accessible at: https://www.kaggle.com/code/avrahamcalev/time-series-models-pamap2-dataset, also under the CC BY 4.0 license, requiring attribution for any use. No additional data were generated during the current study.

Received: 15 November 2025; Accepted: 27 February 2026
Published online: 23 March 2026

References

1. Bowler, N. Eddy-current nondestructive evaluation. *Springer New. York*. https://doi.org/10.1007/978-1-4939-9629-2 (2019).
2. Machado, M. A. Eddy Currents Probe Design for NDT Applications: A Review. *Sensors* **24**, 5819. https://doi.org/10.3390/s24175819 (2024).
3. Xia, Z. et al. Eddy Current Testing for Measuring Planar Structures. *Sensors* **22**, 8695. https://doi.org/10.3390/s22228695 (2022).
4. Trung, L. Q. *Development of Eddy Current Probes Based on Various Core Shapes and Materials*. Doctoral dissertation, Department of Artificial Environment Graduate School of Environment and Information Sciences Yokohama National University. (2024).
5. Trung, L. Q., Kasai, N., Sekino, K. & Miyazaki, S. Eddy current convergence probes with self-differential and self-nulling characteristics for detecting cracks in conductive materials. *Sens. Actuators A: Phys.* **349**, 114084. https://doi.org/10.1016/j.sna.2022.114084 (2023).
6. Chen, T. et al. Design and performance research of a new dual-excitation uniform eddy current probe. *Sensors* **22**, 8850. https://doi.org/10.3390/s22228850 (2022).
7. Repelianto, S. A. & Kasai, N. The improvement of flaw detection by the configuration of uniform eddy current probes. *Sensors* **19** (2), 397. https://doi.org/10.3390/s19020397 (2019).
8. Mirzaei, M., Ripka, P. & Grim, V. A novel eddy current speed sensor with a ferrite E-core. *IEEE Mangn. Lett.* **11**, 1–5. https://doi.org/10.1109/LMAG.2020.2993501 (2020).
9. Tytko, G. Eddy current testing of conductive coatings using a pot-core sensor. *Sensors* **23** (2), 1042. https://doi.org/10.3390/s23021042 (2023).
10. Vasić, D., Rep, I., Špikić, D. & Kekelj, M. Model of magnetically shielded ferrite-cored eddy current sensor. *Sensors* **22** (1), 326. https://doi.org/10.3390/s22010326 (2022).
11. Zhao, L., Lyu, Y., Liu, F., Liu, Z. & Zhao, Z. Experimental Investigation on the Effect of Coil Shape on Planar Eddy Current Sensor Characteristic for Blade Tip Clearance. *Sensors* **24** (18), 6133. https://doi.org/10.3390/s24186133 (2024).
12. Song, M., Li, M., Xiao, S. & Ren, J. Research on the influence of geometric structure parameters of eddy current testing probe on sensor resolution. *Sensors* **23** (14), 6610. https://doi.org/10.3390/s23146610 (2023).
13. Xie, Y. et al. A novel conductivity measurement method for non-magnetic materials based on sweep-frequency eddy current method. *IEEE Trans. Instrum. Meas.* **71**, 1–12. https://doi.org/10.1109/TIM.2022.3188538 (2022).
14. Huang, P. et al. Decoupling conductivity and permeability using sweep-frequency eddy current method. *IEEE Trans. Instrum. Meas.* **72**, 1–11. https://doi.org/10.1109/TIM.2023.3242017 (2023).
15. Hachi, D. et al. Numerical investigation to study the influence of thickness and electrical conductivity of metal-sheets on the LOI-Point of a PEC sensor. *Nondestructive Test. Evaluation*. **39** (4), 886–904. https://doi.org/10.1080/10589759.2023.2232930 (2024).
16. Meng, B., Zhuang, Z., Ma, J. & Zhao, S. Study on the effect of pulsed eddy current lift-off characteristics for feeding metallic foreign objects detection in coal mine crushers. *Sci. Rep.* **15** (1), 23775. https://doi.org/10.1038/s41598-025-08185-x (2025).
17. Meng, B., Zhuang, Z., Ma, J. & Zhao, S. Research on the detection method for feeding metallic foreign objects in coal mine crushers based on reflective pulsed eddy current testing. *Appl. Sci.* **14** (24), 11704. https://doi.org/10.3390/app142411704 (2024).
18. Sophian, A., Tian, G. & Fan, M. Pulsed eddy current non-destructive testing and evaluation: A review. *Chin. J. Mech. Eng.* **30** (3), 500–514. https://doi.org/10.1007/s10033-017-0122-4 (2017).
19. Chen, X. & Lei, Y. Electrical conductivity measurement of ferromagnetic metallic materials using pulsed eddy current method. *Ndt E Int.* **75**, 33–38. https://doi.org/10.1016/j.ndteint.2015.06.005 (2015).
20. Desjardins, D., Krause, T. W. & Clapham L Transient eddy current method for the characterization of magnetic permeability and conductivity. *NDT E Int.* **80**, 65–70. https://doi.org/10.1016/j.ndteint.2016.02.010 (2016).
21. Xia, Z. & Jia, J. Non-Destructive Eddy Current Testing System Based on Discrete Wavelet Transform. *Electronics* **14** (16), 3239. https://doi.org/10.3390/electronics14163239 (2025).
22. Shao, Q., Fan, S. & Liu, F. Parameter optimisation of wavelet denoising for pulsed eddy current signals based on particle swarm optimisation algorithm. *Nondestructive Test. Evaluation*. **39** (5), 1210–1224. https://doi.org/10.1080/10589759.2023.2249583 (2024).
23. Huang, S., Hong, M., Lin, G., Tang, B. & Shen, S. A. Discrete Fourier Transform-Based Signal Processing Method for an Eddy Current Detection Sensor. *Sensors* **25** (9), 2686. https://doi.org/10.3390/s25092686 (2025).
24. Munir, N., Huang, J., Wong, C. N. & Song, S. J. Machine learning based eddy current testing: A review. *Results Eng.* **103724** https://doi.org/10.1016/j.rineng.2024.103724 (2024).
25. Pérez, E. et al. Integrating AI in NDE: techniques, trends, and further directions. *NDT E Int.* **103442** https://doi.org/10.1016/j.ndteint.2025.103442 (2025).
26. Smetana, M., Behun, L., Gombarska, D. & Janousek, L. New proposal for inverse algorithm enhancing noise robust eddy-current non-destructive evaluation. *Sensors* **20** (19), 5548. https://doi.org/10.3390/s20195548 (2020).
27. Zuo, Y. et al. Multi-Modal Joint Pulsed Eddy Current Sensor Signal Denoising Method Integrating Inductive Disturbance Mechanism. *Sensors* **25** (12), 3830. https://doi.org/10.3390/s25123830 (2025).
28. Le, M. et al. Enhancing corrosion detection in pulsed eddy current testing systems through autoencoder-based unsupervised learning. *NDT E Int.* **146**, 103175. https://doi.org/10.1016/j.ndteint.2024.103175 (2024).

29. Kucheryavskiy, S., Egorov, A. & Polyakov, V. Coupling analytical models and machine learning methods for fast and reliable resolution of effects in multifrequency eddy-current sensors. *Sensors* **21** (2), 618. https://doi.org/10.3390/s21020618 (2021).
30. Halchenko, V. Y., Trembovetska, R., Tychkov, V. & Kovtun, V. Robust parameter design of eddy current meters for the electrical conductivity of materials and products of considerable thickness. *Measurement* **119218** https://doi.org/10.1016/j.measurement.2025.119218 (2026).
31. Halchenko, V. Y., Trembovetska, R., Tychkov, V. & Kovtun, V. Robust Parameter Design of Eddy Current Measuring Devices for Magnetic Permeability of a Moving Strip of Ferromagnetic Rolled Metal. *J. Nondestruct Eval*. **45** (12). https://doi.org/10.1007/s10921-025-01295-6 (2026).
32. Halchenko, V., Trembovetska, R. & Tychkov, V. Robust parameter design of surface eddy current probes. The case of measuring geometric anomalies in a stationary test object. *Tekhnichna Elektrodynamika*. **5**, 76–88. https://doi.org/10.15407/techned2025.05.076 (2025).
33. Halchenko, V. Y., Trembovetska, R. V. & Tychkov, V. V. Application of Taguchi Method in Design of Surface Eddy Current Probes for Diagnostics of Power Equipment. *Problemele energeticii regionale*. **64** (4), 10–20. https://doi.org/10.52254/1857-0070.2024.4-64.02 (2024).
34. Zhang, S. & Ida, N. Calculation model for the induced voltage in rectangular coils above conductive plates. *Facta Universitatis Series: Electron. Energetics*. **30** (1), 27–38. https://doi.org/10.2298/FUEE1701027Z (2016).
35. Zhang, S. & Ida, N. Analytical calculation of induced voltages of uniform eddy current probes above a moving conductor. In *International Conference on Sensing and Imaging*, Cham: Springer International Publishing 177–193 (2017)., June https://doi.org/10.1007/978-3-319-91659-0_13
36. Krishnaiah, K. & Shahabudeen, P. *Applied design of experiments and Taguchi methods* (PHI Learning Pvt. Ltd., 2012).
37. Real Statistics Using Excel. Available: https://real-statistics.com/design-of-experiments/taguchi-design-of-experiments/5-level-taguchi-designs/
38. Montgomery, D. C. *Design and analysis of experiments*. Wiley (July 2022).
39. Aslett, L. J., Coolen, F. & De Bock, J. Uncertainty in engineering: introduction to methods and applications. *Springer Nat.* https://doi.org/10.1007/978-3-030-83640-5 (2022).

Acknowledgements

The author is grateful to all colleagues and institutions that contributed to the research and made it possible to publish its results.

Author contributions

Conceptualization, H.V.; methodology, H.V.; software, H.V.; validation, T.R.; and T.V.; formal analysis, T.R.; investigation, H.V.; resources, T.V.; data curation, T.R.; writing—original draft preparation, H.V.; writing—review and editing, H.V. and T.R.; visualization, T.V.; supervision, T.V. All authors have read and agreed to the published version of the manuscript.

Declarations

Competing interests

The authors declare no competing interests.

Additional information

Correspondence and requests for materials should be addressed to V.T.